Netsu Sokutei **33** (3) 114-126

解　説

Calorimetric/*PVT* Investigations of the Interactions in Polymer/Gas Systems under High Pressures☆

Séverine A. E. Boyer

(Received April 6, 2006; Accepted May 20, 2006)

Materials selection is usually made according to their thermophysical and structural properties. To provide a useful guide to the utilization of materials in a given set of conditions (temperature *T*, pressure *P* and pressurizing conditions), *PVT*-Controlled scanning calorimetry named scanning transitiometry permits to well document phase diagrams. The type and extent of {polymer/gas} interactions as well as thermophysical properties are obtained from thermal and mechanical measurements resulting from the methodology controlling precisely the temperature and pressure. Scanning transitiometry permits to scan one of the independent variables (*P*, *V*, or *T*) while the other independent variable is kept constant. Simultaneous change of the dependent variable is recorded together with the associated thermal effect. The effect of pressure on the thermophysical properties, especially using carbon dioxide as a pressurizing fluid, is investigated along two types of runs. *P*ressure-Controlled Scanning Calorimetry (*P*CSC) run is employed to determine the global cubic thermal expansion coefficients‡ of semicrystalline polymers in interaction with a fluid. *T*emperature-Controlled Scanning Calorimetry (*T*CSC) run is employed to investigate the isotropic transitions of amphiphilic liquid crystalline di-block copolymers under a pressurizing fluid. These polymers play an essential role as regards the safety of transport of petroleum products and are promising candidates as templates for microelectronics and biotechnology.

1. Introduction

Petroleum industries[1-3] and nano-science with advanced nano-technologies[4-8] require the knowledge of interfacial phase behaviour between polymers and gaseous molecules. The design and construction of new process plants and equipments are expensive and demanding exercises which should not be jeopardized by the use of inaccurate data.[9,10] The phase equilibrium behaviour of polymer/gas system, particularly at elevated temperatures and pressures, must be well documented. Likewise, numerous methods have been developed to describe the equilibrium condition, with the choice of different equations to describe the properties of the components making up the system under investigation. Meaningful theoretical progress cannot be made, however, without experimental data of the highest accuracy.

The first research of thermal behaviour was

☆ Dedicated to Prof. Jean-Pierre E. GROLIER on the Occasion of his 70th Birthday, theme 'International Symposium of Thermodynamic of Complex Fluids'. The event is associated to the 40th Anniversary of AFCAT (French Association of Calorimetry and Thermal Analysis) during the JCAT37 (37th Calorimetric and Thermal Analysis Days, June 2006, Pau, France).

‡ The expression 'global cubic thermal expansion coefficient' derives from thermal effects developed both in the polymer itself and in the sorption/desorption process of a supercritical fluid in the course of isothermal pressure variations.

introduced by Henry Le Châtelier in 1887, on clay minerals by the heating curve method. In the same way, the similar research was conducted by Gustave Tammann and in 1905 he coined the term 'Thermische Analyse' well-known as "Thermal analysis". Nowadays, thermal analysis is largely used, not only in research but also in development and applications such as standardization and pharmacopoeia. Thermal analysis when coupled with an other technique extends its domain of investigations and becomes more informative, like for example thermogravimetry with differential thermal analysis (TG-DTA) or DSC with DSC-X ray diffractometry[11] or high-pressure CO_2 differential thermal analysis DTA equipments,[12-14] high-pressure differential scanning calorimetry (HP-DSC),[15,16] and scanning transitiometry (ST) set up.[17-23]

Scanning transitiometry combines the benefits of thermal analysis and of *PVT* method; it possesses a large range of applications. Exploration is made under programmed temperature or pressure control; and the data, thermal and mechanical outputs, are simultaneously recorded. As an example, it can be used to describe phase equilibria in asymmetric binary systems under pressure like (tetracosane + methane).[24] It permits to document the efficient porosity of compounds during isothermal compression/decompression cycles on heterogeneous lyophobic systems made of a porous, solid matrix in presence of a nonwetting liquid; such systems are expected to be used as mechanical devices to store, dissipate or transform mechanical energy.[25] In the field of applied polymer science, Grolier *et al* have shown the advantages of scanning transitiometry; three different applications are described namely, determination of thermophysical properties of polymers pressurized either by a non compressible inert fluid (mercury) or by highly compressible gases (CO_2), effect of pressure on different phase transitions (glass transition, fusion/crystallization), and one-line monitoring fine particles synthesis.[26]

In the present paper, an other utilization of scanning transitiometry is presented when using carbon dioxide as pressure transmitting fluid under rigorous control of pressure and temperature. The aim of this study is the *in-situ* analysis of heat flux due to {polymer/gas} interactions when a polymer is submitted simultaneously to barometric and chemical constraints generated by high-pressure CO_2. From this, discussion of pressure effect in selected thermoplastic semicrystalline polymers and amphiphilic liquid crystalline di-block copolymers with an emphasis on thermodynamic aspect is possible; it is focused on how the interactions are influenced depending on the physicochemical state of carbon dioxide either as a gas (GCO_2) or a liquid (LCO_2) or as a supercritical fluid ($SCCO_2$). Measurements have been made along *P*ressure-Controlled Scanning Calorimetry (*P*CSC) run. Different thermodynamico-thermal differential detection modes were developed taking full advantage of the differential mounting of experimental cells, namely the thermal II differential comparative mode and the thermal II differential mode.† Qualitative and quantitative analyses of heat of interactions of medium-density polyethylene (MDPE) and poly(vinylidene fluoride) (PVDF) during sorption/desorption process have been made along isotherms, under pressure jumps, as well as under pressure and volume scans. Similar measurements have been made along *T*emperature-Controlled Scanning Calorimetry (*T*CSC) run according to the thermodynamico-thermal I differential mode.† (**Figs.1-2**). Isotropic transitions in amphiphilic liquid crystalline di-block copolymers PEO_m-*b*-$PMA(Az)_n$ and liquid crystalline homopolymer $PMA(Az)_n$ have been analyzed along isobars under temperature scans.

2. Methods and Materials

2.1 Methods

Simultaneous investigation of both thermal (calorimetry) and mechanical (*PVT* principle) effects describes scanning transitiometry. The technique is called transitiometry from latin transitio (or change) and greek *με'τρον* (or measure) because it permits direct study

† Thermodynamico-thermal II differential mode: the measuring cell contains the polymer sample while the reference cell contains an inert-metal (stainless steel) sample. In the case of the comparative mode, a polymer sample is placed in the reference cell. The samples are identical in size and volume. Both cells are connected to the fluid-pressurizing line.
Thermodynamico-thermal I differential mode: the measuring cell contains the polymer sample in contact with the hydrostatic pressurizing fluid while the reference cell acts as a thermal reference cell, i.e. it is not connected to the fluid-pressurizing line.

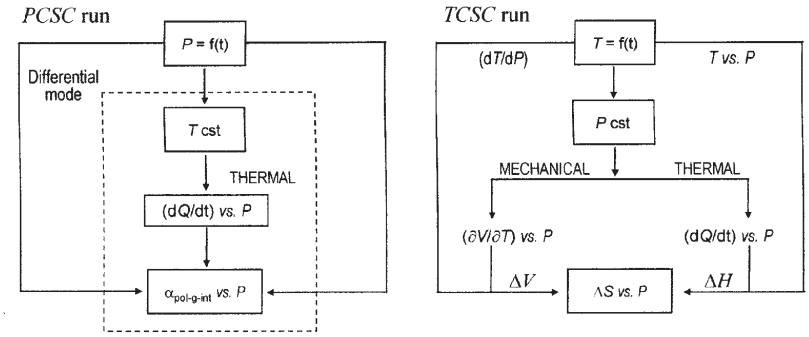

Fig.1 Schematic view of the *PVT*-controlled scanning calorimetry with the *P*ressure-Controlled scanning calorimetry (*P*CSC) run and the *T*emperature-Controlled scanning calorimetry (*T*CSC) run.

of physicochemical transitions of various types and a much deeper description than could be done with separate calorimetric and/or dilatometric analysis.[19] The apparatus was designed by Randzio of the Institute of Physical Chemistry of the Academy of Science in Warsaw, Poland.[17] Calorimetric experiments were made at the Laboratory of Thermodynamics of Solutions and Polymers, Blaise-Pascal University, Clermont-Ferrand (France). The high pressure calorimeter (ST, type BGR TECH model ST-5VI, Warsaw, Poland) is designed to be operated under hydrostatic pressures up to 400 MPa.[26] It is possible to select different pressurizing fluids, like for example mercury (Hg), or nitrogen (N_2) or difluoro-ethylene ($C_2H_2F_2$), or carbon dioxide (CO_2)···. The block diagram of the system was schematically illustrated in reference.[27] An oil pump coupled to a maximator compressor (a booster) is used to generate hydrostatic pressure when using gases. Pressure is transmitted to the calorimetric detector cell via a high pressure line. Pressure is detected by a 400 MPa (Viatran 0-60000 psig) gauge and is displayed directly on a digital manometer with an accuracy of 0.15 % (full scale). The resolution of the volumetric system is $(5.24 \pm 0.04)\ 10^{-6}$ cm^3 per motor step. A Labview environment permits to record simultaneously the *P*, *V* and *T* data as well as the associated thermal signals.

The technique involves closed systems (closed cells) and change of the thermodynamic state results from a variation of the inducing independent variable. As it is possible to control precisely the variation of one of the independent variables (pressure *P*, volume *V* or temperature *T*) while the other independent variable remains constant, the *PVT*-controlled scanning calorimetry can be operated in different scanning situations as depicted **Fig.1**. In the present work, according to the specific purpose two runs are used.

In the isothermal *P*ressure-Controlled scanning calorimetry (*P*CSC) situation the pressure is taken as the inducing variable and varied as a linear or stepwise function of time. By means of a stepping motor pump driving the hydraulic line, both pressure and volume are monitored and programmed. The calorimeter records the differential heat flow between the respective measuring and reference cells. Simultaneous recording of both differential heat flow and volume changes resulting from a given pressure variation under isothermal conditions leads to the determination of $(\partial S/\partial P)_T$ or by virtue of Maxwell's relation leads to the cubic thermal expansivity α_P as a function of pressure. Pressure steps or jumps at constant temperature are advantageously used, for instance, for observing equilibrium with pressure dependence. In the isobaric run named *T*emperature-Controlled scanning calorimetry (*T*CSC) the temperature is taken as the inducing variable and varied as a linear or stepwise function of time.[28] Simultaneous recording of both differential heat flow and volume changes resulting from a given temperature variation under isobaric conditions leads to the simultaneous determination of both $(\partial H/\partial T)_P$ and $(\partial V/\partial T)_P$ as a function of temperature at a given pressure. Constant rate heating is suitable to survey the sample thermal behaviour in a wide temperature range under different hydrostatic pressures.

2.2 Materials

Extruded polyolefins semicrytalline polymers used are medium-density polyethylene, MDPE (Finathene 3802) crystallinity 49 % and poly(vinylidene fluoride), PVDF

(Kynar 50HD) crystallinity 48 %. The glass transition temperature (T_g) is, respectively, 163 and 235 K; the melting temperature (T_m), respectively, 400 and 441 K. Because of their final use (as materials for making pipelines), commercial polymer samples were supplied by French Institute of Petroleum (IFP). *P*CSC run is performed on cylindrical rod samples of dimensions 75.0 mm in height and 4.4 mm in diameter having a relatively small mass, *i.e.* about 1.0 g for MDPE and 1.9 g for PVDF. The measurements are taken from 353 to 403 K and pressure up to 100 MPa of CO_2 and N_2.

Amphiphilic liquid crystalline di-block copolymers PEO_m-*b*-$PMA(Az)_n$ consist of two chemically different blocks, namely hydrophilic semicrystalline sequences of poly(ethylene oxide), PEO_m, and hydrophobic sequences of polymethacrylate derivative containing mesogene azobenzene units, 11-[4-(4'-butylphenyl-azo)phenoxy]-undecyl methacrylate, $PMA(Az)_n$. Di-block copolymers PEO_m-*b*-$PMA(Az)_n$ were prepared by atom transfer radical polymerization, *m* and *n* indicate the degree of polymerization of PEO and PMA(Az) components, respectively.[29-32] Four phase transitions are ascribed to the melting of PEO, the melting of azobenzene moieties PMA(Az), the smectic and the isotropic transitions. In the case of PEO_{114}-*b*-$PMA(Az)_{20}$ the transitions temperatures are, respectively, 312, 337, around 368 and 388 K. Because of connectivity/incompatibility constraints between the two blocks, PEO_m-*b*-$PMA(Az)_n$ spontaneously self-assemble into microphase-separated nanometer-sized domains that exhibit high ordered hexagonal packed PEO cylinders structures. As an example PEO_{114}-*b*-$PMA(Az)_{46}$ shows dense periodic arrays of PEO cylinders with diameters of 11.8 ± 0.2 nm and a distance between cylinders of 19.8 ± 0.4 nm. *T*CSC run is performed on copolymers in the form of a powder placed in an open glass ampoule. Amphiphilic di-block copolymers PEO_{114}-*b*-$PMA(Az)_{20}$, with the respective weights of 0.1967 and 0.3845 g, were investigated under CO_2 and Hg as pressure media. PEO_{114}-*b*-$PMA(Az)_{40}$ sample with a weight of 0.1052 g was investigated under CO_2. For comparison, the liquid crystalline homopolymer $PMA(Az)_{30}$ with a weight of 0.2143 g was investigated under Hg. The measurements were taken at pressure up to 50 MPa during isotropic transition over the temperature range from 380 to 420 K.

In these measurements, polymers are always in intimate contact with the pressure transmitting fluids. Both gases, carbon dioxide (purity of 99.5 %) and nitrogen (purity of 99.95 %), were supplied by SAGA France and used without further purification. Respectively, the critical pressure and temperature for CO_2 and N_2 are (7.38 MPa, 3.40 MPa) and (304.13 K, 126.19 K). In these conditions, CO_2 is either in the gas state (GCO_2) or in the supercritical state ($SCCO_2$); N_2 is in the supercritical state (SCN_2). Hg was used as a chemical inert pressure transmitting fluid and preferred due to its well-known thermomechanical coefficients ($\alpha_P = 1.80\ 10^{-4}\ K^{-1}$ and $\kappa_T = 0.40\ 10^{-4}\ MPa^{-1}$).

Thermal with energetic calibrations of the calorimetric detector were performed with the melting of three standard organic substances: *p*-chlorobromobenzene, *p*-dibromobenzene and benzoic acid. The temperature and enthalpy of fusion are, respectively, (337.73 K[33], 360.45 K[33], 395.52 K[34]) and (97.99 J g^{-1}, 87.03 J g^{-1}, 147.90 J g^{-1}).[35]

3. Results and discussion

3.1 Pressure-Controlled Scanning Calorimetry PCSC

The calorimetric detector measures the differential heat flux (between reference and measuring cells) resulting from the physicochemical effects occurring during the sorption (fluid-pressurizing pressure)/desorption (fluid-depressurizing pressure) process. According to the respective role of the measuring and reference cells (**Fig.2**) the thermal II differential mode was selected, described as the thermal II differential comparative mode and as the thermal II differential mode with a reference (**Fig.2(a)-(b)**). For each thermal II mode, the measured heat rate with polymer was corrected for the heat effects produced by pressurization/depressurization of the hydraulic fluid (expansibility) and the volume sample (unsymetry of the equipment) through appropriate blank experiments. Under identical conditions of *T* and *P*, and under the assumption that there were no interactions between the metallic rod and the gas, blank experiments were performed where replacing the polymer sample with a metal-stainless steel sample of identical dimensions.[27,36]

Isothermal investigations of interactions were made on polymers kept in the solid state, *i.e.* between glass and melting transitions. Two gases were selected for their different properties: essentially N_2 being less polar than CO_2 is considered as more 'neutral' when interacting with the polymers. As well as, experiments with high-pressure

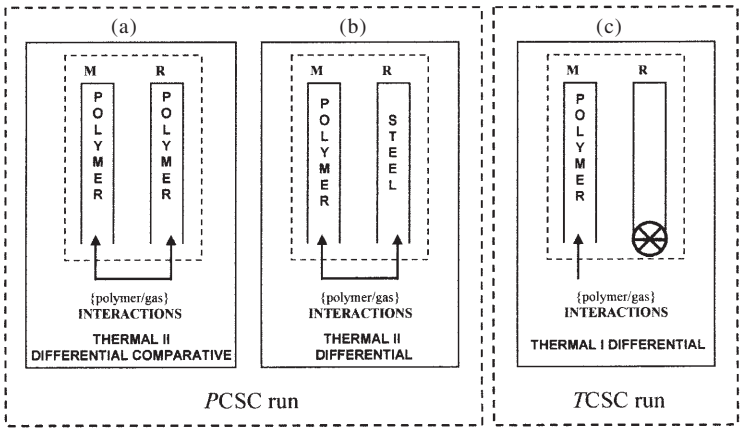

Fig.2 *PVT*-controlled scanning calorimetry including the calorimetric detector equipped with high-pressure cells and a supercritical *PVT* line. According to the respective role of the measuring M and reference R cells, three thermal modes are described. In *P*CSC run, (a) thermal II differential comparative mode, where both measuring and reference cells contain a polymer and are connected to the gas line; (b) thermal II differential mode, where the measuring cell contains the polymer and the reference cell contains an inert sample of equal volume, both cells are connected to the gas line. In *T*CSC run, (c) thermal I differential mode, where the measuring cell contains the polymer and is connected to the gas line while the reference cell acts as a thermal reference.

Hg permits to decouple hydrostatic pressure effects from solvent solubility effects.

Thermal II differential comparative mode: MDPE and PVDF at 372 K

An original use based on their respective role, of the measuring and reference cells, permits essentially to directly decouple hydrostatic pressure effects from heats effects between {MDPE/CO_2} and {PVDF/CO_2}. The thermal II differential comparative mode was experimented where a MDPE sample is placed in the measuring cell while a PVDF sample is placed in the reference cell. The two samples being identical in size and volume, both cells were connected to the gas line (**Fig.2(a)**). Each sample placed in one of the two calorimetric cells is simultaneously submitted to the same conditions, *i.e.* to the same barometric (pressure change), thermal (372.59 K) and chemical (CO_2) environments. The calorimetric signal, *i.e.* the comparative {(MDPE-PVDF)/CO_2} differential heat flux (**Fig.3**), is then proportional to the thermal effect due to the difference of the {polymer/gas} interactions between the two polymers. The data are corrected through blank experiments. Series of calorimetric measurements are collected under step-wise pressure variations between 0.1 and 100 MPa.

A first study was made during continuous pressure scans in function of time as represented in **Fig.3(a)**, where simultaneous thermal (heat flux) and mechanical (linear volume change dV) effects are recorded; it shows that the comparative heat flux becomes exothermic around 40 MPa. A second study with three different types of fluid-pressurizing modes was made as represented in **Fig.3(b)**: pressures jumps comprised between 6 and 28 MPa, volume scans with a change of the calorimetric active volume of $dV = 1.364$ cm^3 (with a rate of about 11.10^{-4} cm^3 s^{-1}) and pressure scans with a change of the pressure $dP = 15$ MPa (with a rate of about 45.10^{-4} MPa s^{-1}). Isotherms of CO_2-pressurization and of CO_2-depressurization were performed in order to investigate possible hysteresis between sorption and desorption. Data are given in W per pressure unit. Below 40 MPa, calorimetric signal is endothermic with $dQ\{$(MDPE-PVDF)/$CO_2\}/dP < 0$, thus PVDF exhibits higher interactions with CO_2 than MDPE. Above 40 MPa the reverse situation is observed, calorimetric signal becomes exothermic with $dQ\{$(MDPE-PVDF)/$CO_2\}/dP > 0$, showing that the differential heat flux of interactions for {MDPE/CO_2} becomes larger than for {PVDF/CO_2}.

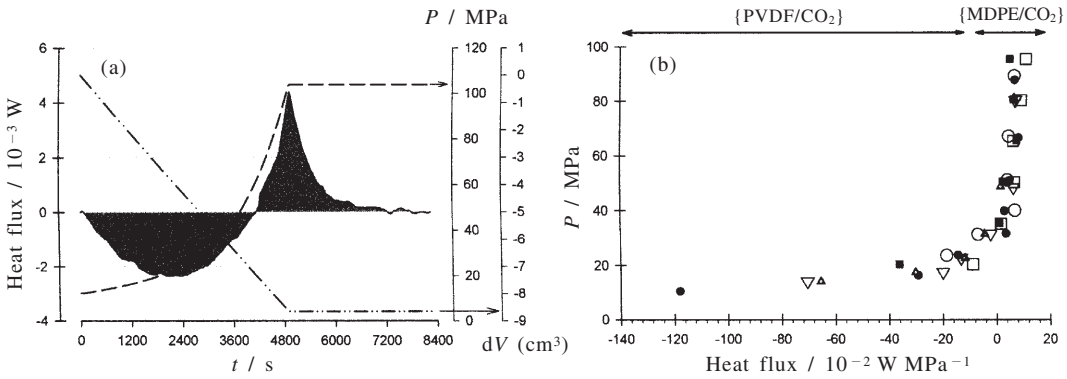

Fig.3 Thermal II differential comparative heat flux dQ(MDPE-PVDF) under CO_2 at 372.59 K. (a) Measurements were taken during continuous pressure scan in function of time. (b) Measurements were taken along either compression (closed symbols) or decompression (open symbols), and during either pressure jumps (circles) or volume scan (triangles) or pressure scan (squares).

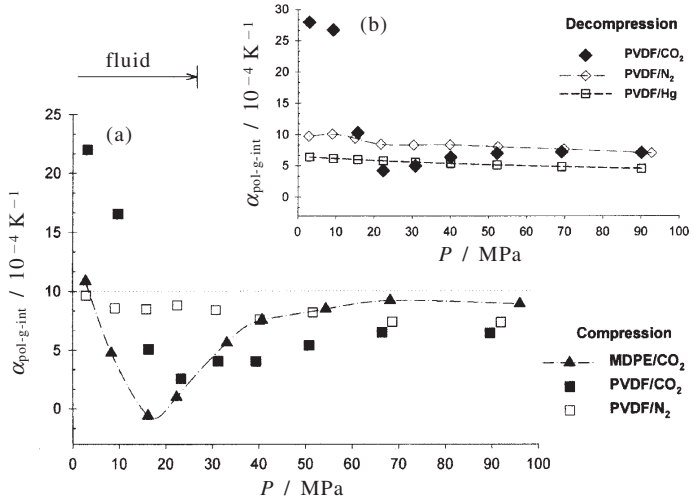

Fig.4 Global cubic thermal expansion coefficients $\alpha_{pol\text{-}g\text{-}int}$ of gas-saturated PVDF and MDPE, obtained with the thermal II differential mode under CO_2 and N_2 at 372.02 K, during compression and decompression pressure jumps. The graph on the bottom left-hand side shows the variation of $\alpha_{pol\text{-}g\text{-}int}$ of MDPE and PVDF with CO_2 and N_2, respectively, during compression. The graph on the top right-hand side shows the variation of $\alpha_{pol\text{-}g\text{-}int}$ of PVDF with CO_2, N_2 and Hg, respectively, during decompression.

Thermal II differential mode with reference sample: MDPE and PVDF at 372 K under pressure jumps

In the thermal II differential mode, the polymer sample is placed in the measuring cell while an inert reference of equal volume is placed in the other (reference) cell, both cells being connected to the gas line which serves to pressurize (**Fig.2(b)**). The thermal effect of {polymer/gas}, resulting from the interaction, is quantitatively represented through the calculated global cubic thermal expansion coefficients $\alpha_{pol\text{-}g\text{-}int}$ of the gas-saturated polymer. The coefficient is calculated from the determination of the heat involved during pressure change and by virtue of the appropriate Maxwell's relation; a detailed description is given in reference.[27] Evolution with pressure at 372.02 K of $\alpha_{pol\text{-}g\text{-}int}$ for both MDPE and PVDF depending on the pressurizing fluid, that is

{MDPE/CO_2}, {PVDF/CO_2}, {PVDF/N_2}, {PVDF/Hg}, respectively, during pressure jumps is represented in **Fig.4**.

Heat flux of interactions (exothermic CO_2-pressurization and endothermic CO_2-depressurization) exhibit a minimum at about 20 MPa. The heat flux minimum is reflected in the isotherms of $\alpha_{pol\text{-}g\text{-}int}$ coefficients of CO_2-saturated polymer at about 18 and 25 MPa, respectively, for MDPE and PVDF, in contrary to what is observed with N_2 and Hg for which the isotherms of interactions are 'monotonous' (**Fig.4(a)**). At low pressures below 30 MPa, more energetic interactions are observed with PVDF compared to MDPE; that is demonstrated by larger global $\alpha_{pol\text{-}g\text{-}int}$\{PVDF/$CO_2$\}. Above 30 MPa, the global $\alpha_{pol\text{-}g\text{-}int}$\{MDPE/$CO_2$\} overpasses the global $\alpha_{pol\text{-}g\text{-}int}$\{PVDF/$CO_2$\}; this means stronger interactions in the case of MDPE. These results confirm the more energetic CO_2-interactions observed when using the thermal II comparative differential mode. As shown in **Fig.4(b)**, N_2 acts as a 'relatively neutral' fluid but with higher interactions than Hg and with smaller interactions than CO_2. The heat effects reflects a small sorption and parallels the remarkable plasticization efficiency of nitrogen in polystyrene, particularly at elevated pressure.[37] The PVDF values during depressurization's steps under CO_2 and/or N_2 are similar; what is consistent as regards the reversibility of the sorption/desorption phenomena.[36]

The cubic expansion coefficient of gas-saturated polymer is substantially affected by the CO_2 in the supercritical state as indicated by the minimum of $\alpha_{pol\text{-}g\text{-}int}$ observed with MDPE/CO_2 and PVDF/CO_2 systems. The dependency of $\alpha_{pol\text{-}g\text{-}int}$ coefficients with the physical state of the pure gas, *i.e.* a minimum corresponding in a mirror-image to the maximum in the temperature dependence of α_p for pure CO_2 gas, is a striking feature of the above investigation. It clearly shows the influence of gas sorption on the thermophysical properties of the polymers. In semicrystalline polymers, it seems that lower pressures most probably induce a first adsorption of CO_2 with a sorption by the amorphous part and in some interstitial sites; while higher pressures induce the absorption into the whole polymer matrix, with a mechanical distension, into a pseudo-homogeneous state, that leads to a supercritical-saturated polymer.

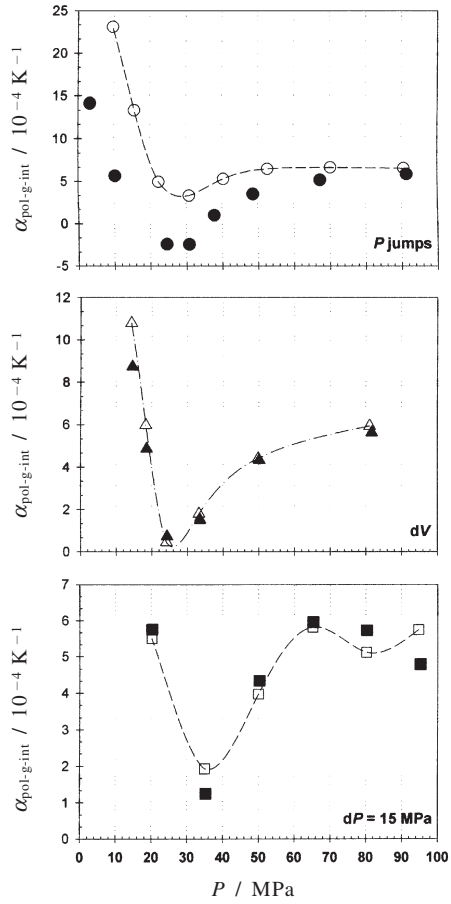

Fig.5 Global cubic thermal expansion coefficients $\alpha_{pol\text{-}g\text{-}int}$ of saturated PVDF investigated with the thermal II differential mode under CO_2 at 401.50 K during compression (closed symbols) or decompression (open symbols), of pressure jumps (circles) or volume scans (triangles) or pressure scans (squares).

Thermal II differential mode with reference sample: PVDF at 402 K under *P* jumps and (*P*, *V*) scanning modes

More information can be obtained from measurements under pressure jumps and during volume and pressure scans on PVDF at 401.50 K. The heats of interactions measured as functions of volume and of pressure go through shallow minima in the 20-40 MPa region; this is illustrated by the trends shown by the thermodynamic coefficient $\alpha_{PVDF\text{-}g\text{-}int}$ under either CO_2 *P* jumps, or *V* or *P* scans, as represented in **Fig.5**.

Results for *V* or *P* scans are similar and show a

good reproducibility, a slight shift of the minimum appears between 15 and 30 MPa. The differences are more marked with *P* jumps. The uncertainties may be essentially due to the manner with which the pressure changes are transmitted to the investigated sample. During an abrupt change of pressure, the system is thermodynamically thrown off balance, whereas transitiometry is a technique which yields optimal response at the thermodynamic equilibrium where Maxwell's relations can apply. Most likely, the small shift of the minimum toward higher pressures in the case of *V* scans compared to *P* jumps would be a consequence of the relaxation of the system which reaches a more stable state under thermodynamic equilibrium. The formation of a micro-organized domain is probably generated in the amorphous phase of the polymer. It may also correspond to a "competitive" equilibrium between plasticization effect and hydrostatic effect of CO_2 in the polymer. In addition, the minimum would mean that {polymer/supercritical gas} interactions are favoured. Gas sorption, *i.e.* easiness of CO_2 impregnation by the polymer, results in the reduction of the molecular forces between polymer chains inducing thus an increase of free volume in the polymer matrix, *i.e.* concomitant swelling.[36,38,39)]

Conclusion on PCSC run with the thermal II differential mode

From the above results it is observed that plasticization/hydrostatic effect result in a minimum in the relationship between $\alpha_{\text{pol-g-int}}$ and pressure. The pressure for MDPE is slightly smaller that those of PVDF. Below 30 MPa and compared to MDPE, interactions with PVDF are more energetic. Both polymers having the same degree of crystallinity (X_c of 50 %) the higher energy can be preferred by the presence of fluoride in pure PVDF, *i.e.* the strong polar C-F bonds may give high dipolar interactions with the polarizable CO_2. Then higher energetic interactions of PVDF would suggest that incorporation of CO_2 in PVDF (sorption with plasticization effect) is stronger than in MDPE.[40)] This is confirmed by high pressure measurements which show that highly condensed systems, like PVDF/CO_2, have a smaller thermal expansion coefficients than for less condensed systems, like MDPE/CO_2.[41)] The thermal data are corroborated by results obtained with a 'weighing' technique using a vibrating wire sensor and coupled with a *PVT* three cell principle (VW-*PVT*); the data of sorption and swelling obtained with quite different and complementary techniques satisfactorily confirmed the transitiometric results.[36)]

3.2 Temperature-Controlled Scanning Calorimetry TCSC

According to the respective differential principle of the instrument, *i.e.* measuring and reference cells, the thermal I differential mode was chosen (**Fig.2(c)**). The measuring cell contains the polymer sample. The reference cell is not connected to the pressure line and acts only as a thermal reference, thus reducing the thermal noise and the base line shift coming from external perturbations. The systems PEO_m-*b*-$PMA(Az)_n$/CO_2 and PEO_m-*b*-$PMA(Az)_n$/Hg are selected to differentiate the competitive sorption and hydrostatic effects, and to obtain information on molecular interactions in focusing on the behaviour of PMA(Az) with PEO. At isotropic transition, PEO is already a liquid compressed to equilibrium state whereas PMA(Az) passes from a liquid crystalline to a liquid state in equilibrium under pressure. Additionally, the thermal behaviour of amphiphilic liquid crystalline di-block copolymer was compared with the one corresponding to the liquid crystalline homopolymer.

Thermal I differential mode: PEO-*b*-PMA(Az) under *T* scan

Polymer samples are submitted to the triple effects: barometric with the CO_2-pressurizing fluid maintained at constant pressure, chemical by using CO_2 as pressurizing fluid, and thermal by choosing to scan the temperature. Under constant CO_2-hydrostatic pressures from 0.1 to 50 MPa, investigations are performed over the isotropic transition at slow heating rates, *i.e.* 0.2 K min^{-1} with {PEO_m-*b*-$PMA(Az)_n$/CO_2} and {$PMA(Az)_{30}$/Hg} and 0.1 K min^{-1} with {PEO_{114}-*b*-$MPa(Az)_{20}$/Hg}. The slow heating rates permits to keep the system closed to the thermodynamic equilibrium. The pressure is kept constant by monitoring the volume change of the system. As shown in **Fig.6(a)**, the transitiometric curve during isotropic transition of {PEO_{114}-*b*-$PMA(Az)_{40}$/CO_2} at 2 MPa represents the simultaneous thermal (heat flux) and mechanical (volume change shown in steps) effects. The onset temperature is accepted as the isotropic transition temperature (T_{iso}); the transition volume (ΔV_{iso}) and entropy (ΔS_{iso}) are evaluated from mechanical and thermal outputs, respectively. Using CO_2, insights into

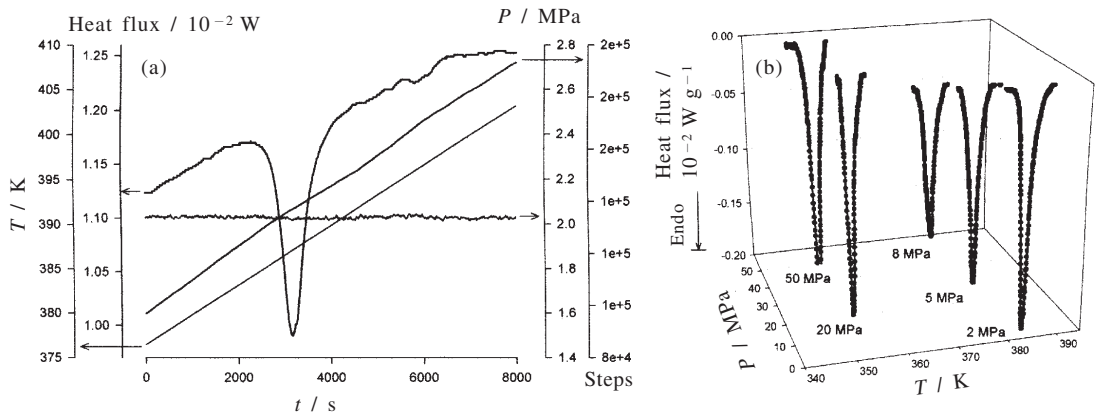

Fig.6 Isobaric representation using the thermal I differential mode over the isotropic transition of {PEO_{114}-*b*-$PMA(Az)_{40}/CO_2$} during heating scans at 0.2 K min^{-1}. (a) Investigations are conducted through the isotropic transition (heat flux) at constant pressure (P), the pressure is kept constant through the volume change (volume change shown in steps) of the system. (b) Measurements are taken from 0.1 to 50 MPa, the pressure effect on the isotropic temperature in the presence of supercritical CO_2 shows a depression in the pressure range of 10 MPa.

the thermophysical properties of the polymer, *i.e.* two phase diagrams (T_{iso}, ΔS_{iso}) *versus P*, are obtained from the thermal output.[42,43)]

PVT-controlled scanning calorimetric heating curves under CO_2 pressures show an endothermic peak as represented in **Fig.6(a)-(b)**; the same pattern was observed with DSC curves under N_2 at 0.1 MPa. Scanning transitiometry investigates *in-situ* the effect of a pressurizing fluid on the transition, effectively the thermal responses give a clear relation between the isotropic temperature and CO_2 pressures. Investigations conducted on PEO_{114}-*b*-$PMA(Az)_{40}$ under CO_2 from 0.1 to 50 MPa show a depression of the isotropic transition in the pressure range up to 10 MPa. The trend is and was verified through the heat flux of PEO_{114}-*b*-$PMA(Az)_{20}$ measured after three successive temperature scans under CO_2 each at 5 and 8 MPa.[42,44)] The differences observed at these two pressures were related to the physical state of CO_2. In the gaseous state (GCO_2, 5 MPa) the variation of T_{iso} was shifted to lower temperature by about 3 K, whereas in the supercritical state ($SCCO_2$, 8 MPa) T_{iso} was practically not changed. This means that the thermodynamic equilibrium is already established during the first run in $SCCO_2$ and is attained more easily than using GCO_2.

The illustration of the behaviour of the isotropic transition under hydrostatic pressure of 'active' CO_2 compared to what observed under pressure of 'inert' Hg is given in **Fig.7**. Hg measurements were obtained in the same way; a detailed description is given elsewhere.[43,45,46)] A quite different variation of T_{iso} and ΔS_{iso} *versus P* is observed with CO_2 and Hg, respectively, in **Fig.7(a)** and **(b)**.

When pressurizing with 'active' CO_2, CO_2 depresses the isotropic temperature and the shift shows a linear variation at low pressures, up to 10 MPa. The variation of the isotropic transition temperature becomes smaller with increasing pressure. T_{iso} tends to a constant value of 355 K at higher pressures, up to 50 MPa, as shown with {PEO_{114}-*b*-$PMA(Az)_{40}/CO_2$} in **Fig.7(a)**. The trend is quite different to that under Hg. When pressurizing with 'inert' Hg, the isotropic temperature increases continuously with pressure. The linear shift corresponding to {PEO_{114}-*b*-$PMA(Az)_{20}$/Hg} is calculated directly through the Clapeyron's equation slope ($\Delta T_{iso}/\Delta P$), e.g. 0.35 K MPa^{-1}, over the pressure range from 0.1 to 50 MPa. For comparison, the same tendency of T_{iso} of liquid crystalline homopolymer $PMA(Az)_{30}$ under Hg is observed. The coefficient of the linear shift is 0.39 K MPa^{-1}. The increase of T_{iso} with Hg reflects the molecular motions restricted by the hydrostatic pressure. The high pressure limits the degrees of freedom of the molecules. The

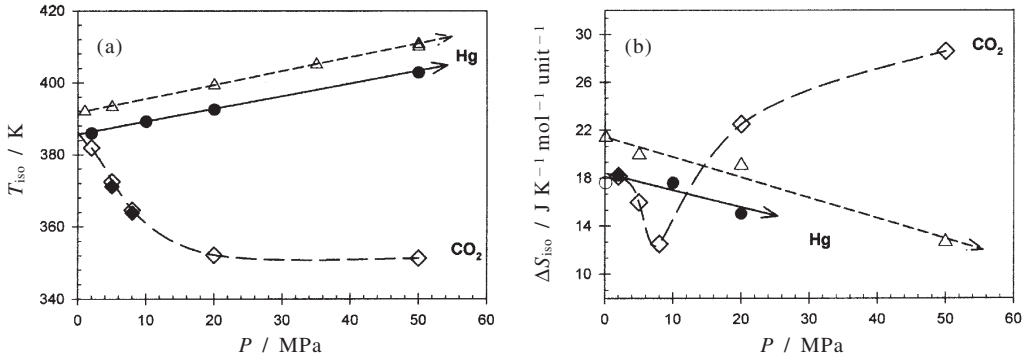

Fig.7 Behaviour of the isotropic transition depending on the hydrostatic pressure of either 'active' CO_2 or 'inert' Hg. (a) Isotropic temperature T_{iso} trend for PEO_{114}-*b*-$PMA(Az)_{20}$ under either CO_2 (closed diamonds) or Hg (closed circles). The trend for {PEO_{114}-*b*-$PMA(Az)_{40}$/CO_2} is displayed at high pressures up to 50 MPa (open diamonds), as well as for {$PMA(Az)_{30}$/Hg} for comparison (open triangles up). (b) Isotropic entropy ΔS_{iso} trend of {PEO_{114}-*b*-$PMA(Az)_{40}$/CO_2} (open diamonds) and of {PEO_{114}-*b*-$PMA(Az)_{20}$/Hg} (closed circles). For comparison, {$PMA(Az)_{30}$/Hg} is displayed at high pressures up to 50 MPa (open triangles up). Data at 0.1 MPa come from DSC investigations on a series of homopolymer $PMA(Az)_{n=20,\ 30,\ 60,\ 139}$ and di-block copolymers $PEO_{m=114}$-*b*-$PMA(Az)_{n=18\ to\ 100}$ under N_2 and under heating rate 10 K min^{-1}, using a DSC 6200 Seiko Instrument In., Japan. The values are given per unit n of degree of $PMA(Az)_n$ polymerization.

isotropic transition of LC homopolymer seems more sensitive to the pressure.

The activity of compressed CO_2 above its critical temperature (304 K, 7.4 MPa), is likely to be changed continuously by changing the pressure from GCO_2 (5 MPa) to $SCCO_2$ (8 MPa). Relative low-pressure CO_2 below 10 MPa facilitates the sorption of the fluid into the copolymer, resulting in a plasticization effect. The supercritical fluid acts as a 'lubricant' between the molecular chains.[47] Since there is an increase in freedom of motion of copolymer chains, the higher ability to orient yields the decrease of T_{iso}. In this scheme, the PEO part is dissolved in $SCCO_2$ and the interface, *i.e.* junction point, between chain end of PEO and methacrylate PMA(Az) acquires molecular mobility. At higher $SCCO_2$ pressures above 10 MPa, the hydrostatic effect overcomes the plasticization effect. The CO_2-saturated polymer is in an environment of high pressure and yields to the stabilization of the isotropic state. It seems that the T_{iso} behaviour reflects the sorption of gas into the polymer with the concomitant volume change. The increase of solubility and swelling occurs first at low pressure, then plasticization levels off and the restriction of molecular motion appears at high pressure.

As illustrated in **Fig.6(b)**, the amplitude of the isotropic transition passes through a minimum around 8 MPa. The quantitative representation of the entropy ΔS_{iso} reflects simultaneously the variations of the enthalpy, *i.e.* integration of heat curves, with the temperature as a function of CO_2 and Hg pressures as represented in **Fig.7(b)**. Clearly, the lowering of the isotropic entropy in the presence of dissolved CO_2 at pressure below 10 MPa is similar to the effect observed on T_{iso}. But on the contrary above 10 MPa, ΔS_{iso}, after a minimum, is shifted to higher values. T_{iso} and ΔS_{iso} seem to vary linearly according to the Clapeyron's equation below 10 MPa. If we compare the same copolymer PEO_{114}-*b*-$PMA(Az)_{20}$ under CO_2 and Hg, the slope $d\Delta S_{iso}/dP$ gives, respectively, -0.72 and -0.18 J K^{-1} mol^{-1} MPa^{-1}, that shows the strong dependence of ΔS_{iso} with CO_2. The dissolved gas reduces the intermolecular interactions, and induces more degree of freedom. The large depression of ΔS_{iso} at 8 MPa is the result of two contributions: entropy of azobenzene at the isotropic transition and mixing entropy ΔS_{mixing} of azobenzene (with polymer part) with CO_2. Then, CO_2 in the gas state (GCO_2, 5 MPa) appears as a 'poor' solvent whereas in the supercritical state ($SCCO_2$, 8 MPa) becomes a more efficient solvent and ΔS_{mixing} becomes smaller. This indicates that the extent of entropy loss depends strongly on the pressure medium. Around 10 MPa, competition appears between plasticization and hydrostatic effects.

Above 10 MPa, the antiplasticization effect of the CO_2-hydrostatic pressure yields to an increase of the entropy. The pressure dependence permits to control the 'easiness' of molecular interactions: {polymer/CO_2} interactions are higher than {polymer/Hg} interactions. In {PEO_{114}-*b*-$PMA(Az)_{20}$/Hg}, the interactions of polymer/liquid crystal system are favoured by the hydrostatic pressure effect. By comparison, the tendency is also demonstrated by the investigations on {$PMA(Az)_{30}$/Hg} with a continuous decrease of ΔS_{iso} up to 50 MPa. The homopolymer has a larger ΔS_{iso} compared to copolymer. The surplus of "isotropic" energy was found to be due to a molecular disturbance located at the interface where much more heat is required because azobenzene part has to overcome the interfacial restriction in the presence of liquid PEO.[43] In the case of {PEO_{114}-*b*-$PMA(Az)_{20}$/CO_2}, the interactions of polymer/gas system are predominantly favoured in presence of $SCCO_2$. The hydrostatic effect by Hg influences the 'physical interactions' between PEO polymer and PMA(Az) liquid crystalline moieties; while when the pressure is exerted by CO_2 the gas not only imposes an hydrostatic effect but also acts as an active solvent which penetrates the molecular organization, *i.e.* penetrates into the block copolymer, and maybe preferably interacts with the PEO polymer part.[48]

Conclusion on TCSC run with the thermal I differential mode

In {PEO_m-*b*-$PMA(Az)_n$/gas}, it is observed the coexistence of a selective interaction-sorption effect between polymer PEO and liquid crystalline part PMA(Az), of an antiplasticization effect and also of the role of the interface between PEO and PMA(Az). Under high-pressure CO_2, because T_{iso} is still observed and stays stable, the liquid crystalline part must be in a CO_2-saturated state with a small CO_2 concentration, concentration which does not disturb the molecular interface. Because mesogenic groups are chemically linked with PEO polymer chains, the increase of ΔS_{iso} might be probably due to the selective sorption into PEO. Oxyethylene groups of PEO blocks plays an important role and the ability of $SCCO_2$ to modify the copolymer interfacial self-organization through more efficient hydrophilic {PEO/$SCCO_2$} interactions was confirmed by atomic force microscopy AFM.[42,49] The di-block copolymer PEO_{114}-*b*-$PMA(Az)_{46}$ was investigated after treatment at 313 and 351 K, respectively, under 9 MPa of CO_2 during 1 hour exposure. Under the $SCCO_2$ treatment, the PEO cylinders kept the hexagonal structure array with an increase in diameter of the nano-tubes. Expansion of the PEO cylinders was due to the absorption of $SCCO_2$ with increasing temperatures.

4. Conclusion

Thermodynamic is essential not only for elucidating characteristics of specific binding but also for predicting the thermodynamic characteristic of systems under different conditions. The ability of scanning transitiometry gives strong experimental bases for discussing selective interactions between polymers and different pressurizing fluids. Polymers can be investigated in the solid or molten states and by choosing to perform calorimetric measurements under either pressure scans or temperature scans, respectively. *P*CSC run in the thermal II differential comparative mode with the thermal II mode, and *T*CSC run in the thermal I differential mode, using CO_2- or Hg- pressurized fluids, permit to decouple polymer/fluid interactions effects from heats effects. The competition between the solubility/plasticization effect and of hydrostatic pressure effect of a fluid in the polymer-rich phase is evidenced, as well as the effect of the interface in the copolymer. The transitiometric *in-situ* {polymer/gas} interactions results were confirmed by consistent data obtained from quite different "weighing" and microscopic techniques. Such combination of experimental data, on same systems, generated by different methods and techniques provides highly valuable information for material selection and industrial applications.[50]

Acknowledgements

This research was initiated in cooperation with the Laboratory of Thermodynamics of Solutions and Polymers (LTSP, Blaise-Pascal University, France) under the direction of Prof. Jean-Pierre E. Grolier (LTSP, Clermont-Ferrand). The author gratefully acknowledges support for this research by a French CIFRE grant project on "The Explosive Decompression Failure Mechanism of Thermoplastic semicrystalline polymers in presence of dissolved gas" with the French Institute of Petroleum (IFP, France) under the directions of Research Directors Mrs. Marie-Hélène Klopffer (IFP, Paris) and Mr. Joseph Martin (IFP, Lyon); and by a Japanese CREST-JST grant

Principal notations used

MDPE	Medium-density polyethylene
PVDF (or PVF_2)	Poly(vinylidene fluoride)
PEO	Poly(ethylene oxide)
PMA(Az)	Polymethacrylate derivative containing mesogene azobenzene units, 11-[4-(4'-butylphenyl-azo)phenoxy]-undecyl methacrylate
LC	Liquid crystal
$SCCO_2$ and GCO_2	Supercritical and gas carbon dioxide, respectively
*P*CSC	Pressure-Controlled Scanning Calorimetry
*T*CSC	Temperature-Controlled Scanning Calorimetry
T_{iso} (K)	Isotropic temperature
ΔS_{iso} (J K^{-1} mol^{-1})	Isotropic entropy
$\alpha_{pol\text{-}g\text{-}int}$ (K^{-1})	Global cubic thermal expansion coefficient

project on "The Creation and Transcription of Reliable Macromolecular Templates based on Phase-separated Nano-structures" under the directions of Research Director Prof. Tomokazu Iyoda (Tokyo Institute of Technology TIT, Tokyo) and of Prof. Hirohisa Yoshida (Tokyo Metropolitan University TMU, Tokyo). Interest and advice of Prof. S. L. Randzio (Institute of Physical Chemistry, Polish Academy of Sciences, Warsaw, Poland) at different stages of this research is highly appreciated.

References

1) B. Dewimille, J. Martin, and J. Jarrin, *J. Phys. IV* **3**, 1559 (1993).
2) R. Scheichl, M-H. Klopffer, Z. Benjelloun-Dabaghi, and B. Flaconnèche, *J. Memb. Sci.* **254**, 275 (2005).
3) N. Von Solms, N. Zecchin, A. Rubin, S. I. Andersen, and E. H. Stenby, *Eur. Polym. J.* **41**, 341 (2005).
4) M. Park, C. Harrison, P. M. Chaikin, R. A. Register, and D. H. Adamson, *Science* **276**, 1401 (1997).
5) R. Coontz and P. Szuromi, *Science* **290**, 1523 (2000).
6) T. Thurn-Albrecht, J. Schotter, G. A. Kästle, N. Emley, T. Shibauchi, L. Krusin-Elbaum, K. Guarini, C. T. Black, M. T. Tuominen, and T. P. Russell, *Science* **290**, 2126 (2000).
7) M. Lazzari and M. A. López-Quintela, *Adv. Mater.* **15**, 1583 (2003).
8) J. J. Chiu, B. J. Kim, E. J. Kramer, and D. J. Pine, *J. Am. Chem. Soc.* **127**, 5036 (2005).
9) S. M. S. Neiro and J. M. Pinto, *Computers and Chemical Eng.* **28**, 871 (2004).
10) M. Tansey and B. Stembridge, *World Patent Information* **27**, 212 (2005).
11) *Comprehensive Handbook of Calorimetry & Thermal Analysis*, Michio Sorai Editor-in-Chief, The Japan Society of Calorimetry and Thermal Analysis, Wiley Editions (2004).
12) A. Seeger, D. Freitag, F. Freidel, and G. Luft, *Thermochim. Acta* **424**, 175 (2004).
13) Y. Maeda, T. Mabuchi, and J. Watanabe, *Thermochim. Acta* **266**, 189 (1995).
14) Y. Maeda, T. Niori, J. Yamamoto, and H. Yokoyama, *Thermochim. Acta* **428**, 57 (2005).
15) S. Zhu, A. Le Bail, and H. S. Ramaswamy, *J. Food Eng.* **75**, 215 (2006).
16) Z. Zhang and Y. P. Handa, *J. Polym. Sci.: Part B: Polym. Phys.* **36**, 977 (1998).
17) S. L. Randzio, J-P. E. Grolier, J. Zaslona, and J. R. Quint, French patent 9109227, Polish patent 295285. Site http://www.transitiometry.com.
18) S. L. Randzio, J-P. E. Grolier, and J. R. Quint, *Rev. Sci. Instrum.* **65**, 960 (1994).
19) S. L. Randzio, *Chem. Soc. Rev.* **25**, 383 (1996).
20) S. L. Randzio, *Thermochim. Acta* **300**, 29 (1997).
21) S. L. Randzio and J-P. E. Grolier, *Anal. Chem.* **70**, 2327 (1998).
22) S. L. Randzio, *J. Therm. Anal. Cal.* **57**, 165 (1999).
23) S. L. Randzio, *Thermochim. Acta* **355**, 107 (2000).
24) S. L. Randzio, C. Stachowiak, and J-P. E. Grolier, *J. Chem. Thermodyn.* **35**, 639 (2003).
25) L. Coiffard, V. A. Eroshenko, and J-P. E. Grolier, *AIChE J.* **51**, 1246 (2005).
26) J-P. E. Grolier, F. Dan, S. A. E. Boyer, M. Orlowska, and S. L. Randzio, *Int. J. Thermophys.* **25**, 297 (2004).
27) S. A. E. Boyer, S. L. Randzio, and J-P. E. Grolier, *J. Polym. Sci.: Part B: Polym. Phys.* **44**, 185 (2006).
28) M. J. O'Neill, *Anal. Chem.* **36**, 1238 (1964).
29) K. Watanabe, Y. Tian, H. Yoshida, S. Asaoka,

and T. Iyoda, *Trans. Materials Res. Soc. Jpn.* **28**, 553 (2003). T. Iyoda, project director, site http://www.res.titech.ac.jp.
30) Y. Tian, K. Watanabe, X. Kong, J. Abe, and T. Iyoda, *Macromolecules* **35**, 3739 (2002).
31) H. Yoshida, K. Watanabe, R. Watanabe, and T. Iyoda, *Trans. Materials Res. Soc. Jpn.* **29**, 861 (2004).
32) H. Yoshida, *Netsu Sokutei* **31**, 234 (2004).
33) A. N. Campel and C. A. Prodan, *J. Am. Chem. Soc.* **70**, 553 (1948).
34) R. J. L. Andon and J. E. Connett, *Thermochim. Acta* **42**, 241 (1980).
35) J. Narbutt, *Elektrochem.* **24**, 339 (1918).
36) S. A. E. Boyer, M-H. Klopffer, J. Martin, and J-P. E. Grolier, *J. Appl. Polym. Sci.*, accepted.
37) S. A. E. Boyer and J-P. E. Grolier, *Pure Appl. Chem.* **77**, 593 (2005).
38) O. Lorge, B. J. Briscoe, and P. Dang, *Polymer* **40**, 2981 (1999).
39) A. R. Berens, G. S. Huvard, R. W. Korsmeyer, and F. W. Kunig, *J. Appl. Polym. Sci.* **46**, 231 (1992).
40) S. A. E. Boyer, J. Martin, F. Dan, and J-P. E. Grolier, Calcon - The 58th Calorimetry Conference Session IIIA: Materials, Communication 《William F. Giauque Memorial Award》 (2003).
41) S. L. Randzio, *Phys. Lett.* **117**, 473 (1986).
42) S. A. E. Boyer, J-P. E. Grolier, L. Pison, C. Iwamoto, H. Yoshida, and T. Iyoda, CATS 2005, issue *J. Therm. Anal. Cal.*, in press.
43) S. A. E. Boyer, J-P. E. Grolier, H. Yoshida, and T. Iyoda, *J. Polym. Sci.: Part B: Polym. Phys.*, submitted.
44) S. A. E. Boyer, L. Pison, C. Iwamoto, J-P. E. Grolier, H. Yoshida, and T. Iyoda, *Polymer Preprints Japan* **2**[54], 3215 (2005).
45) S. A. E. Boyer, J-P. E. Grolier, H. Yoshida, and T. Iyoda, *Polymer Preprints Japan* **1**[54], 815 (2005).
46) H. Yoshida, T. Yamada, R. Watanabe, K. Watanabe, T. Iyoda, T. Delrieu, and J-P. E. Grolier, IUPAC World Polymer Congress Macro - 40th International Symposium on Macromolecules Proceedings 2.3.3: Polymers in the solid state (2004).
47) A. F. Ismail and W. Lorna, *Sep. Purif. Technol.* **27**, 173 (2002).
48) H. Lin and B. D. Freeman, *J. Molecular Structure* **788**, 250 (2006).
49) S. A. E. Boyer, J-P. E. Grolier, and T. Yoshida, Pacifichem Communication Session 86: Carbon dioxide-based Processes for Polymer Synthesis/ Processing, Microelectronics, and Nanoscale Manufacturing (2005).
50) A. R. C. Duarte, L. E. Anderson, C. M. M. Duarte, and S. G. Kazarian, *J. Supercritical Fluids* **36**, 160 (2005).

要　旨

材料をその使用目的に応じて的確に選択するには，その構造ならびに熱物性が重要な意味を持つ。圧力・体積・温度制御熱容量測定（scanning transitiometry）によって得られる相図は，温度，圧力，圧力媒体などの様々な条件下における材料選択を行うための基礎データとして有用である。Scanning transitiometry では，一定温度での圧力走査（*P*CSC）ならびに一定圧力での温度走査（*T*CSC）によって，転移エンタルピーと転移体積を測定することが可能である。さらに様々な気体を圧力媒体として利用することで，熱物性データに加えて高分子－気体間相互作用に関する情報を得ることができる。二酸化炭素を圧力媒体として用いた場合の熱物性に対する圧力依存性を，原油輸送の安全性に関係する二種類の結晶性高分子（中密度ポリエチレン，ポリフッ化ビニリデン）の*P*CSC 測定による体積膨張係数の評価と，*T*CSC 測定による液晶型両親媒性ブロック共重合体の等方性転移を例に解説した。

Séverine A. E. BOYER
*Dept. of Applied Chemistry, Graduate School of Engineering, Tokyo Metropolitan Univ., e-mail: boyer@comp.metro-u.ac.jp
**Lab. of Thermodynamics of Solutions and Polymers, Blaise Pascal Univ., Clermont-Ferrand, France e-mail: severine.boyer@univ-bpclermonf.fr
***CREST-Japan Science and Technology Agency